

# Neutrino Emission and Plasma Heating from Primordial Black Holes: An Improved Approach to $N_{\text{eff}}$ Constraints

Héctor Sanchis<sup>1</sup>, Gabriela Barenboim<sup>1</sup>, Yuber F. Perez-Gonzalez<sup>2</sup>

<sup>1</sup>Departament de Física Teòrica and IFIC, Universitat de València-CSIC, E-46100, Burjassot, Spain

<sup>2</sup>Departamento de Física Teórica and Instituto de Física Teórica UAM/CSIC, Universidad Autónoma de Madrid, Cantoblanco, 28049 Madrid, Spain

E-mail: [hector.sanchis@uv.es](mailto:hector.sanchis@uv.es), [gabriela.barenboim@uv.es](mailto:gabriela.barenboim@uv.es), [yuber.perez@uam.es](mailto:yuber.perez@uam.es)

**Abstract.** We investigate the impact of neutrino emission via Hawking radiation from primordial black holes (PBHs) on the cosmological effective number of neutrino species,  $N_{\text{eff}}$ , after neutrino decoupling. By comparing this effect with observational limits, we derive bounds on the abundance of light PBHs. Our analysis incorporates two previously unaccounted-for effects: the emission of secondary neutrinos from unstable particles, which increases  $N_{\text{eff}}$ , and the modification of the neutrino-photon temperature ratio due to particle emission heating the photon plasma, which lowers  $N_{\text{eff}}$ . Overall, including these effects allows us to impose constraints on PBH masses with initial masses in the range  $10^9 \text{ g} \lesssim M_{\text{ini}} \lesssim 10^{13} \text{ g}$ . However, our limits remain less stringent than those derived from Big Bang Nucleosynthesis.

---

## Contents

<b>1</b>	<b>Introduction</b>	<b>1</b>
<b>2</b>	<b>A short review on PBHs</b>	<b>2</b>
<b>3</b>	<b>Bounds from <math>N_{\text{eff}}</math></b>	<b>4</b>
3.1	Numerical calculation of the bounds	8
<b>4</b>	<b>Results</b>	<b>9</b>
<b>5</b>	<b>Conclusions</b>	<b>13</b>
<b>Appendix A Energy-dependent neutrino interactions</b>		<b>14</b>
<b>Appendix B Calibration of the spectra</b>		<b>15</b>

---

## 1 Introduction

Black holes have been a subject of scientific interest for over a century, yet many fundamental questions about them remain unresolved. While the formation of stellar-mass black holes from the collapse of massive stars is well understood, the origin of the supermassive black holes observed at the centers of galaxies remains an open question [1].

It is possible that black holes formed in the early universe, giving rise to what are known as primordial black holes (PBHs). A key property of black holes is that they are expected to emit thermal radiation [2, 3]. This Hawking radiation includes all degrees of freedom existing in nature. However, only low-mass black holes emit significant amounts of radiation, making the detection of Hawking radiation from known astrophysical black holes unlikely. Light PBHs, if they exist, could emit detectable levels of Hawking radiation. Depending on their initial mass, strong constraints exist on the abundance of PBHs that could have existed or still persist in the Universe [4–6]. These objects have been proposed as a potential explanation for various astrophysical and cosmological mysteries, including the origin of supermassive black holes [1], the nature of dark matter [7–39] and the matter-antimatter asymmetry in the universe [40–58]. Moreover, PBHs could also generate observable gravitational waves [59–63] or other forms of dark radiation [10, 17, 18, 64–67] and affect the stability of the Higgs potential [68–70].

This work explores the impact of Hawking radiation from light PBHs—particularly neutrino emission—on the effective number of relativistic species,  $N_{\text{eff}}$ , and its gravitational effects on the universe. Since these effects are observationally constrained, they provide a means to place bounds on the abundance of light PBHs. Our approach primarily focuses on modifications to the total energy density of neutrinos and photons. However, the injection of high-energy neutrinos could also induce spectral distortions in the Cosmic Microwave Background (CMB). Accurately determining such effects would require solving the Boltzmann equations. While recent studies have introduced novel approaches to address these challenges, see e.g. [71–74], in this work, we restrict our analysis to the impact of PBH evaporation on the total energy density.

This approach has been previously studied in Refs. [10, 17, 18, 64], but here we incorporate additional physical effects that are relevant for neutrino emission after neutrino decoupling. Specifically, we account for: (i) secondary neutrinos produced from the decay of other Hawking-emitted particles, which enhance  $N_{\text{eff}}$  and strengthen the bounds, and (ii) the heating of the photon plasma by non-neutrino Hawking radiation, which modifies the neutrino-photon temperature ratio and weakens the bounds. These effects do not merely shift existing constraints; they also provide deeper insights into the underlying physical processes.

Our results demonstrate that incorporating these effects leads to tighter bounds on PBH abundance through this mechanism, though these constraints remain weaker than those derived from other cosmological probes, such as Big Bang Nucleosynthesis (BBN) [75–78]. Furthermore, we find that heating the cosmic plasma can effectively reduce the measurable gravitational impact of neutrinos, allowing for a greater number of extra neutrinos without violating observational constraints. This insight could have implications beyond the scope of this study.

The paper is structured as follows: Sec. 2 provides a brief overview of PBHs, their Hawking radiation, and existing observational constraints. Sec. 3 details our method for deriving new bounds on PBH abundance and compares it to previous approaches. The resulting bounds are presented and analyzed in Sec. 4. Finally, we summarize our conclusions in Sec. 5. We include two appendices, App. A, where we describe a procedure to determine whether neutrinos from evaporation would interact with the plasma. App. B considers the calibration that we used for the Hawking spectra from BlackHawk [66, 79]. Throughout this work, we adopt natural units ( $\hbar = c = k_B = 1$ ), unless stated otherwise.

## 2 A short review on PBHs

To form black holes with masses significantly smaller than the Chandrasekhar limit, typically associated with astrophysical black holes, it is necessary for overdensities to exceed a critical threshold since in a radiation dominated Universe, the pressure would prevent the gravitational collapse [4, 5]. In general, there are several theoretical scenarios have been proposed to explain how such large density perturbations could develop, leading to the formation of primordial black holes (PBHs). In this work, we assume that a population of PBHs formed due to some unspecified mechanism, and it is characterized by its initial mass,  $M_{\text{in}}$ , i.e., we consider a monochromatic mass distribution, and initial energy density,  $\beta'$ . In an initially radiation-dominated Universe, the initial PBH mass can be related to the plasma temperature as follows,

$$M_{\text{in}} = \frac{4\pi}{3} \gamma \frac{\rho_{\text{rad}}(T_{\text{form}})}{H^3(T_{\text{form}})} \sim 2 \times 10^{12} \text{ g} \left( \frac{\gamma}{0.2} \right) \left( \frac{10^{11} \text{ GeV}}{T_{\text{form}}} \right)^2. \quad (2.1)$$

Here  $\rho_{\text{rad}}$  represents the radiation energy density at the black hole formation temperature  $T_{\text{form}}$ , while  $H$  denotes the Hubble rate, and  $\gamma \sim 0.2$  defines the gravitational collapse factor for a radiation-dominated Universe. Inspecting the Schwarzschild radius for these PBH,

$$r_{\text{S,in}} = 2GM_{\text{in}} \sim 2.7 \times 10^{-5} \text{ fm} \left( \frac{M_{\text{in}}}{10^{10} \text{ g}} \right), \quad (2.2)$$

we observe that these black holes are microscopic, so that we need to consider how quantum effects affect the evolution of these objects.

Building on this fact, and applying a semi-classical approximation in which quantum fields propagate within a classical gravitational field, Hawking [2, 3] demonstrated that black holes emit radiation across all existing degrees of freedom in nature. The differential emission rate per unit energy  $E$ , per unit time  $t$ , for a particle of type  $i$  with mass  $m_i$  is given by

$$\frac{d^2 N_i}{dt dE} = \frac{g_i}{2\pi} \frac{\vartheta(M, E)}{e^{E/T_{\text{BH}}} - (-1)^{2s_i}} \quad (2.3)$$

with  $g_i$  are the internal degrees of freedom of the particle, and, more importantly, the temperature associated to the black hole is

$$T_{\text{BH}} = \frac{1}{8\pi GM} \sim 1 \text{ TeV} \left( \frac{10^{10} \text{ g}}{M} \right), \quad (2.4)$$

where  $M$  is the instantaneous PBH mass. In particular, the dependence of the emission rate on the internal degrees of freedom of the particle implies that the amount of neutrinos emitted as Hawking radiation will depend on whether neutrinos are Dirac or Majorana particles. More specifically, in the Dirac case, the amount of neutrinos that are directly emitted from a black hole (so-called primary neutrinos) will be twice as much as in the Majorana case, due to the presence of right-handed neutrinos. In contrast, neutrinos that come from the decays of other emitted particles (so-called secondary neutrinos) always come from weak decays, which only produce left-handed neutrinos in any case, so their abundance is the same in both cases [64].

The Hawking spectrum in Eq. (2.3) departs from being the spectrum of a blackbody due to the presence of the spin-dependent absorption probability  $\vartheta(M, E)$ . Since the curved spacetime around a black hole effectively acts as a potential barrier, a particle coming from infinity could be either back-scattered or absorbed by the black hole. Such an absorption probability, given by  $\vartheta(M, E)$ , is the same as the probability of an emitted particle to reach spatial infinity.

As real particles are emitted from the black hole's gravitational field, it gradually loses mass. The rate of this mass loss can be estimated by [3, 80, 81]

$$\frac{dM}{dt} = - \sum_i \int_{M_i}^{\infty} \frac{d^2 N_i}{dt dE} E dE = -\varepsilon(M) \frac{1}{G^2 M^2}, \quad (2.5)$$

where  $G$  is the gravitational constant. Here, we have introduced the mass evaporation function  $\varepsilon(M)$ , which captures the degrees of freedom that can be emitted at any given moment, corresponding to the instantaneous mass of the black hole. We adopt the parametrization of this function as outlined in Ref. [22]. Crucially, the estimation above assumes that the gravitational field remains largely unaffected by the emission of a particle. However, this assumption eventually breaks down, requiring consideration of the backreaction to the metric caused by the Hawking emission process. Some studies have incorporated this backreaction using the semi-classical approximation, showing that the mass loss rate still follows the  $M^{-2}$  law as given in Eq (2.5) [82–84].

Thus, naively, one would expect the Hawking spectrum and the mass loss rate equations to remain valid until the black hole's mass reaches the Planck mass [3], where quantum gravity effects should be relevant. Nevertheless, when examining the time evolution of the von Neumann entropy of Hawking radiation alongside the coarse-grained black hole entropy, assumed to match the Bekenstein-Hawking value [85, 86], Page observed that the von Neumann entropy exceeds the black hole's available degrees of freedom at a point known as the

Page time, leading to the information paradox [87–90]. Despite recent progress in addressing the paradox [88], several unresolved questions remain regarding the thermal characteristics of Hawking evaporation beyond the Page time and the potential modifications to the mass loss rate. In light of the uncertainty surrounding these possible alterations, we will assume that the semi-classical approximation holds true up to approximately the Planck scale, enabling the primordial black hole time evolution to conform to the mass loss rate specified in Eq. (2.5).

The second parameter that characterizes the PBH population is the initial energy density  $\rho_{\text{BH}}(T_{\text{form}})$ . Following Ref. [4], we define such initial PBH abundance through the parameter  $\beta'$ , that relates the total and PBH energy densities via

$$\beta' \equiv \gamma^{1/2} \left( \frac{g_{\star}(T_{\text{form}})}{106.75} \right)^{1/4} \frac{\rho_{\text{BH}}(T_{\text{form}})}{\rho_{\text{tot}}(T_{\text{form}})}, \quad (2.6)$$

where  $g_{\star, \text{form}}$  are the relativistic degrees of freedom at formation. Having defined the main parameters that characterize the PBH population, we consider now its time evolution in the Early Universe. Such time evolution will be governed by the Friedmann equation for the comoving energy densities  $\varrho_i = a^{3(1+w_i)}\rho_i$ , with  $w_i$  the equation-of-state parameter for each component,  $i = \{\text{rad}, \text{PBH}\}$  [23, 91, 92]

$$\frac{d\varrho_{\text{rad}}}{dN_e} = -\frac{a}{H} \frac{d \ln M}{dt} \varrho_{\text{PBH}}, \quad (2.7a)$$

$$\frac{d\varrho_{\text{PBH}}}{dN_e} = \frac{1}{H} \frac{d \ln M}{dt} \varrho_{\text{PBH}}, \quad (2.7b)$$

where we have chosen the number of e-folds,  $N_e = \ln(a)$ , where  $a$  is the scale factor, as our time variable, and the Hubble parameter  $H$  is

$$H^2 = \frac{8\pi}{3M_{\text{Pl}}^2} (a^{-4}\varrho_{\text{SM}} + a^{-3}\rho_{\text{PBH}}). \quad (2.8)$$

Given that the PBH population acts as a matter component, PBH domination may occur when [10, 64, 91]

$$\beta' \gtrsim \beta'_c \equiv 2.5 \times 10^{-16} \left( \frac{g_{\star}(T_{\text{form}})}{106.75} \right)^{-1/4} \left( \frac{M_{\text{in}}}{10^{10} \text{ g}} \right)^{-1}. \quad (2.9)$$

Various constraints exist on the parameter space defined by  $\beta'$  and  $M_{\text{in}}$ , depending on whether and when the PBH population evaporated throughout cosmological history [4, 5]. PBHs having  $M_{\text{in}} \gtrsim 10^8 \text{ g}$  are expected to evaporate during the epochs of BBN and CMB formation. Therefore, we can expect strong constraints on the initial PBH abundance for such masses [4, 5, 75–78]. Here, we will consider additional bounds coming from the production of neutrinos that contribute to the number of relativistic degrees of freedom, as constrained by CMB observations.

### 3 Bounds from $N_{\text{eff}}$

Let us begin by reviewing the definition of  $N_{\text{eff}}$  in the context of standard cosmology. Since neutrino decoupling occurs shortly before electron-positron annihilation, the photon plasma

undergoes heating, whereas the neutrino background remains largely unaffected [93]. Consequently, the radiation energy density after annihilation can be expressed as

$$\rho_r = \frac{\pi^2}{30} \left( 2 + \frac{7}{8} 2N_\nu \left( \frac{T_\nu}{T} \right)^4 \right) T^4, \quad (3.1)$$

where  $\rho_r$  denotes the energy density of relativistic species in the universe,  $N_\nu = 3$  represents the number of neutrino species in the SM, and  $T$  ( $T_\nu$ ) corresponds to the photon (neutrino) temperature. More generally, the effective number of relativistic species,  $N_{\text{eff}}$ , is defined as

$$N_{\text{eff}} = \left( \frac{11}{4} \right)^{4/3} \left( \frac{T_\nu}{T} \right)^4 N_\nu. \quad (3.2)$$

Assuming there are no additional sources of neutrinos and considering instantaneous decoupling, the ratio of temperatures is given by  $T_\nu/T = (4/11)^{1/3}$ . However, taking into account the interactions between electrons and neutrinos during electron-positron annihilation, a more precise calculation yields the  $\Lambda$ CDM value of  $N_{\text{eff}}^{\Lambda\text{CDM}} = 3.046$ , see Ref. [94].

Introducing PBHs into the analysis leads to two significant effects:

1. **Particle injection.** The first effect arises from the fact that PBHs emit neutrinos, thereby increasing  $N_\nu$  and, consequently,  $N_{\text{eff}}$ . More formally, since these additional neutrinos contribute to the radiation energy density  $\rho_r$ , they introduce an additional term in Eq. (3.2). This contribution can be effectively absorbed into  $N_{\text{eff}}$ , leading to its enhancement.
2. **Entropy injection.** The second effect comes from PBHs emitting other SM particles, such as photons. If these particles are released after neutrino decoupling but before photon decoupling, their energy is injected into the photon plasma. Since, after neutrino decoupling, the photon plasma is no longer in thermal equilibrium with the neutrino background, this injection preferentially heats the photon plasma relative to the neutrino plasma. As a result, the temperature ratio  $T_\nu/T$  decreases, leading to a reduction in  $N_{\text{eff}}$ , as indicated by Eq. (3.2).

The first effect was used in Refs. [10, 17, 18, 64] to derive constraints on the PBH abundance, considering the effect of the emission of light particles having different spins. Specifically, Ref. [64] considered the case of emission of right-handed neutrinos, after assuming neutrinos to be Dirac particles. By employing Eq. (3.8) from Ref. [64], we account for the first effect while neglecting the second. It is important to note that the second effect can result in  $\Delta N_{\text{eff}} < 0$ , whereas Eq. (3.8) imposes the constraint  $\Delta N_{\text{eff}} \geq 0$ . This approximation remains valid before neutrino decoupling, as the additional emitted photons thermalize with the neutrinos in the plasma, ensuring that the ratio  $T_\nu/T$  remains unaffected after decoupling. However, after neutrino decoupling, these emitted photons influence the temperature ratio and could lead to a decrease in  $N_{\text{eff}}$ , meaning that their contribution can no longer be disregarded.

To determine the modification to  $N_{\text{eff}}$  due to PBH emission after neutrino decoupling, we consider the contribution of an additional dark radiation component,  $\rho_{\text{DR}}$ , to the standard

radiation energy density,

$$\begin{aligned}\rho_r &= \frac{\pi^2}{30} \left( 2 + \frac{7}{8} 2N_\nu \left( \frac{T_\nu}{T} \right)^4 \right) T^4 + \rho_{DR} \\ &= \frac{\pi^2}{30} \left( 2 + \frac{7}{8} 2(N_\nu + N_{DR}) \left( \frac{T_\nu}{T} \right)^4 \right) T^4,\end{aligned}\tag{3.3}$$

where  $N_{DR}$  is defined analogously to the standard neutrino contribution  $N_\nu$  as

$$N_{DR} = \frac{\rho_{DR}}{\rho_r^{\text{SM}}} \left( \frac{8}{7} \left( \frac{T_\nu}{T} \right)^{-4} + N_\nu \right).\tag{3.4}$$

Here,  $\rho_r^{\text{SM}}$  represents the radiation energy density in the Standard Model when no dark radiation is present, i.e.,  $\rho_{DR} = 0$ . This definition follows from the standard expression for  $N_{\text{eff}}$ , as given in Eq. (3.2).

Thus, in the presence of a dark radiation component, the effective number of relativistic species is given by

$$N_{\text{eff}} = \left( \frac{11}{4} \right)^{4/3} \left( \frac{T_\nu}{T} \right)^4 (N_\nu + N_{DR}).\tag{3.5}$$

Substituting the definition of  $N_{DR}$  from Eq. (3.4), we obtain the modified expression for  $N_{\text{eff}}$  that accounts for both additional relativistic degrees of freedom and changes in the radiation temperature:

$$N_{\text{eff}} = \left( \frac{11}{4} \right)^{4/3} \left( \frac{T_\nu}{T} \right)^4 \left( N_\nu + \frac{\rho_{DR}}{\rho_r^{\text{SM}}} \left( \frac{8}{7} \left( \frac{T_\nu}{T} \right)^{-4} + N_\nu \right) \right).\tag{3.6}$$

In this context, the fraction  $\rho_{DR}/\rho_r^{\text{SM}}$  must be evaluated at the moment when we seek to determine  $N_{\text{eff}}$ . If this fraction is known at a different moment, we must translate it to the desired epoch. To first approximation, this ratio evolves primarily due to species annihilations occurring between the two moments, which introduces the usual *effective number of relativistic species* scaling factors, see Ref. [10, 64]. However, this assumption does not hold if there is energy injection between these moments.

In the cases of interest here, the available information corresponds to the epoch when PBHs have just evaporated, whereas the desired moment is the matter-radiation equality. Since PBHs have already fully evaporated during this interval, no additional energy injection is expected, allowing us to apply the standard scaling behavior discussed in Ref. [64]

$$\frac{\rho_{DR}(T_{eq})}{\rho_r^{\text{SM}}(T_{eq})} = \frac{\rho_{DR}(T_{ev})}{\rho_r^{\text{SM}}(T_{ev})} \left( \frac{g_*(T_{ev})}{g_*(T_{eq})} \right) \left( \frac{g_{*S}(T_{eq})}{g_{*S}(T_{ev})} \right)^{4/3},\tag{3.7}$$

where  $T_{eq} \approx 0.8$  eV is the temperature at matter-radiation equality, and  $g_{*S}(T)$  are the entropic relativistic degrees of freedom. Substituting this relation, we obtain the final expression for  $N_{\text{eff}}$ :

$$N_{\text{eff}} = \left( \frac{11}{4} \right)^{4/3} \left( \frac{T_\nu}{T} \right)^4 \left( N_\nu + \frac{\rho_{DR}(T_{ev})}{\rho_r^{\text{SM}}(T_{ev})} \left( \frac{g_*(T_{ev})}{g_*(T_{eq})} \right) \left( \frac{g_{*S}(T_{eq})}{g_{*S}(T_{ev})} \right)^{4/3} \left( \frac{8}{7} \left( \frac{T_\nu}{T} \right)^{-4} + N_\nu \right) \right).\tag{3.8}$$

The first term in this equation corresponds to “effect 2”, arising from a modification in the temperature ratio, which may deviate from its standard value. In the second term, substituting  $T_\nu/T \approx (4/11)^{1/3}$  recovers “effect 1”, which accounts for the additional contribution of dark radiation emitted by PBHs. By refraining from making this substitution, we retain a correction term that slightly reduces the increase in  $N_{\text{eff}}$  due to “effect 1”. This correction emerges from the interplay between both effects: if they had been treated separately and then summed, this correction would not appear.

Using Eq. (3.8), we can compute  $N_{\text{eff}}$  for any given initial PBH mass  $M_{\text{in}}$  and abundance  $\beta'$ . If the resulting value of  $N_{\text{eff}}$  is inconsistent with current observational constraints, we can exclude that particular  $\beta'$  at the given PBH mass. This enables us to place mass-dependent bounds on  $\beta'$  based on this effect. Importantly, since the modification to  $N_{\text{eff}}$  can be either positive or negative, both upper and lower observational limits on  $N_{\text{eff}}$  must be taken into account.

To constrain the effects of PBH evaporation on  $N_{\text{eff}}$ , we consider the observational bounds from Planck related to the measurement of the power spectrum, cross correlations and anisotropies, and the E-mode polarization of the CMB, i.e., the TT, TE, EE+lowE values from in Tab. 4, given in Ref. [95]. We do not include BAO or lensing constraints, as our primary focus is on  $N_{\text{eff}}$  at the time of CMB emission, whereas BAO and lensing constraints primarily probe later cosmic epochs. At the  $2\sigma$  confidence level, these bounds are given by

$$2.55 < N_{\text{eff}} < 3.28. \quad (3.9)$$

Since these constraints apply to  $N_{\text{eff}}$  at the time of CMB emission, we consider only PBHs that have fully evaporated before this epoch. This ensures that their complete contribution to  $N_{\text{eff}}$  is present by the time the CMB was emitted. Consequently, we restrict our analysis to initial PBH masses up to approximately  $2 \times 10^{13}$  g.

To quantify the neutrino emission from PBHs, we analyze both Dirac and Majorana neutrino cases, as the number of emitted neutrinos differs between these scenarios. To account for changes in the neutrino-to-photon temperature ratio due to the emission of other particles, we use the fact that the photon energy density scales as  $\rho_\gamma \propto T^4$ . This allows us to write

$$\left(\frac{T_\nu}{T}\right)^4 = \left(\frac{T_\nu}{T}\right)_{\text{standard}}^4 \cdot \left(\frac{\rho_\gamma^{\text{SM}}}{\rho_\gamma^{\text{SM}} + \rho_\gamma^{\text{PBH}}}\right), \quad (3.10)$$

where  $\rho_\gamma^{\text{SM}}$  is the standard photon energy density and  $\rho_\gamma^{\text{PBH}}$  represents the energy density of photons emitted by PBHs. The standard temperature ratio is given by:

$$\left(\frac{T_\nu}{T}\right)_{\text{standard}}^4 = \left(\frac{4}{11}\right)^{4/3} \frac{N_{\text{eff}}^{\Lambda\text{CDM}}}{3}. \quad (3.11)$$

For full accuracy,  $\rho_\gamma^{\text{SM}}$  should also include photons emitted before neutrino decoupling, as these remain present but do not affect the temperature ratio. This is a small correction but is accounted for in our analysis. The standard photon energy density is given by

$$\rho_\gamma^{\text{SM}} = \frac{\pi^2}{15} T(\beta' = 0)^4, \quad (3.12)$$

where  $T(\beta' = 0)$  denotes the plasma temperature in the absence of PBHs.

An important consideration is that neutrino decoupling occurs approximately one second after the Big Bang. Prior to this, neutrinos and photons remain in thermal equilibrium due to weak interactions. Consequently, any neutrinos or photons emitted before this epoch will thermalize and will not alter the neutrino-photon temperature ratio or their respective energy densities. Therefore, neutrinos and photons emitted before neutrino decoupling can generally be ignored. However, there is a crucial exception: for Dirac neutrinos, half of the emitted primary neutrinos are right-handed, meaning they do not participate in weak interactions and thus do not thermalize. As a result, we include these right-handed neutrinos even if they were emitted before neutrino decoupling.

This consideration significantly impacts the PBH mass range for which our analysis is relevant. The primary effects that we include are the contribution of all emitted neutrinos and the reduction in  $N_{\text{eff}}$  due to additional particle emission. These effects are irrelevant for PBHs that evaporate before neutrino decoupling, as all additional emitted particles thermalize and do not affect  $N_{\text{eff}}$ . Thus, our refined approach is particularly relevant for PBHs evaporating after neutrino decoupling, corresponding to PBH masses greater than  $\sim 10^9$  g. Consequently, we focus our analysis on PBHs with masses above  $10^9$  g. For lower masses, if neutrinos are Dirac particles, the constraints derived in Ref. [64] remain applicable. If neutrinos are Majorana particles, however, no meaningful bounds on  $N_{\text{eff}}$  can be placed at these lower masses.

Additionally, for the active left-handed neutrinos, our approach extends beyond simply discarding those emitted before neutrino decoupling. Since neutrinos emitted from PBHs tend to have higher energies than those in the plasma, their interaction probability is increased, allowing them to remain coupled to the plasma even after neutrino decoupling. We incorporate this effect in an energy-dependent manner by defining an energy-dependent “decoupling” temperature. Specifically, we assume that high-energy neutrinos remain in thermal equilibrium and do not contribute to modifications in  $N_{\text{eff}}$  until the temperature of the universe falls below their corresponding decoupling temperature. More details on this approach are provided in Appendix A.

Another potential effect that could influence our analysis arises from the formation of hot spots around PBHs, as discussed in Refs. [96, 97]. In the early universe, these localized regions of increased temperature could modify our reasoning if neutrinos thermalized before escaping the hot spot. This effect is most relevant at very early times, corresponding to extremely high plasma temperatures. However, we have verified that the plasma temperature at which neutrinos cease to thermalize within the hot spot is significantly higher than the temperature at which neutrinos decouple from the plasma. As a result, these hot spots would only impact neutrinos that we were already disregarding in our analysis. Therefore, it is safe to neglect this effect.

### 3.1 Numerical calculation of the bounds

To numerically compute the bounds on  $N_{\text{eff}}$ , we first determined the spectra of neutrinos emitted by PBHs across a range of masses. For this purpose, we utilized the code `BlackHawk` [66, 79], which calculates the Hawking radiation spectra of black holes. The computed spectra include both *primary* neutrinos, which are directly emitted from the PBH, and *secondary* neutrinos, which originate from the decays of other particles emitted by the PBH. To obtain the secondary spectra, `BlackHawk` relies on precomputed tables generated with the particle physics code `PYTHIA` [98]. In addition to neutrinos, we also used `BlackHawk` to compute the spectra of other emitted particles, particularly photons and electrons, which

contribute to the heating of the plasma. This information is crucial for accurately determining the neutrino-photon temperature ratio, a key quantity required in the calculation of  $N_{\text{eff}}$  using Eq. (3.8). By including both primary and secondary neutrino spectra, as well as the thermal effects of other emitted particles, we ensure a precise evaluation of the impact of PBH evaporation on  $N_{\text{eff}}$ .

To relate the PBH abundance  $\beta'$  to the emitted neutrino spectra for a given mass, we first calibrated the spectra following the procedure outlined in Appendix B. Once calibrated, the spectra were integrated over time to obtain the total neutrino spectrum, accounting for redshifting due to cosmic expansion. The time-dependent scale factor was extracted using the cosmology code `CLASS` [99], which was also employed for cross-checks. We then integrated the total spectra over energy to compute the total energy density of emitted neutrinos. The temperatures and radiation energy densities at PBH evaporation, as functions of PBH mass and  $\beta'$ , were obtained using tables generated with `FRISBHEE` [22, 26, 67].

Our results were derived using two approaches: one relying on the `FRISBHEE` tables (with `CLASS` used only for the scale factor), and another based exclusively on `CLASS` outputs. The latter is expected to be less accurate before electron-positron annihilation but serves as a useful consistency check. Since `CLASS` assumes standard cosmology, our bounds are valid only in the absence of a PBH-dominated phase. However, as shown in Ref. [64], existing constraints already exclude PBH domination in the relevant mass range, ensuring the reliability of our results.

We followed a similar procedure using primary and secondary photon spectra from `BlackHawk` to determine the change in the neutrino-photon temperature ratio. We integrated them over time to obtain the total spectrum and then over energy to compute the injected energy density. In addition to photons, we accounted for electrons and positrons, assuming they thermalize and transfer their energy to the photon plasma. The temperature change was then derived using  $\rho_\gamma \propto T^4$ . With the neutrino energy density and the modified neutrino-photon temperature ratio as functions of  $\beta'$ , we applied Eq. (3.8) to compute  $N_{\text{eff}}$ . By identifying the values of  $\beta'$  that exceed observational constraints, we established exclusion bounds on  $\beta'$  for different PBH masses.

To assess the impact of various physical effects, we computed bounds with and without secondary Hawking radiation, as well as with and without the temperature ratio modification. Since the Dirac/Majorana nature of neutrinos remains unknown, we considered both cases. For PBHs of mass  $M = 10^{11}$  g, using the `CLASS`-only method, we also examined scenarios including graviton emission and Kerr PBHs, both with and without graviton emission. Since gravitons, like neutrinos, are relativistic and weakly interacting, they contribute to  $N_{\text{eff}}$  in the same manner as right-handed neutrinos and are not excluded if emitted before neutrino decoupling.

## 4 Results

In this section, we present our main results: new constraints on the abundance of Schwarzschild PBHs in the mass range from  $10^9$  g to approximately  $2 \times 10^{13}$  g. These constraints arise from incorporating physical effects that have not been previously considered in the literature: the contribution of secondary neutrino emission and the modification of the neutrino-photon temperature ratio due to the entropy injection from Hawking radiation beyond neutrinos.

We first examine the individual impact of two effects mentioned before. Fig. 1 illustrates how the PBH abundance  $\beta'$  affects  $N_{\text{eff}}$  for a Schwarzschild PBH with mass  $M = 10^{11}$

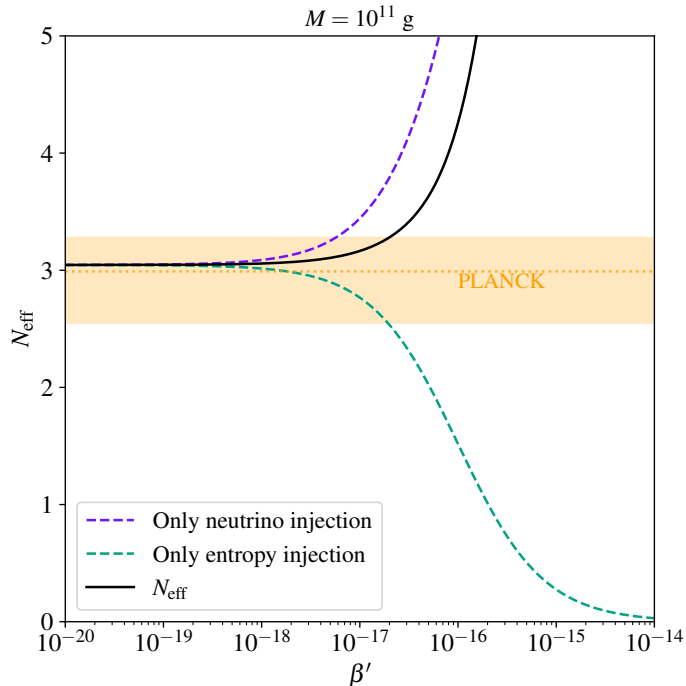


**Figure 1:** Effects of Hawking radiation from Schwarzschild PBHs with mass  $M = 10^{11}$  g on  $N_{\text{eff}}$ , assuming Majorana neutrinos, as a function of PBH abundance  $\beta'$ . The contribution from neutrino emission (purple dashed line) increases  $N_{\text{eff}}$ , while entropy injection reducing the neutrino-photon temperature (green dashed line) lowers it. The total effect (black line) combines both contributions. Observational bounds from Ref. [95] are shown as an orange band.

g, assuming Majorana neutrinos. While the Dirac case would yield slightly different quantitative results, the qualitative behavior remains unchanged, making the following discussion applicable to both cases. The figure separately presents the two competing effects: (i) an increase in  $N_{\text{eff}}$  due to neutrino emission as Hawking radiation (purple dashed) —labeled as *only neutrino injection*— and (ii) a decrease in  $N_{\text{eff}}$  caused by plasma heating from photons and electrons (green dashed) —labeled as *only entropy injection*—, which reduces the neutrino-photon temperature ratio  $T_\nu/T$ . The net change in  $N_{\text{eff}}$ , shown in black, is the sum of these effects. The observational  $2\sigma$  limits from Planck [95] are included in the figure as the orange band. The bound on  $\beta'$  is determined by the point where  $N_{\text{eff}}$  exceeds the upper observational limit—values of  $\beta'$  beyond this threshold are excluded. Notably, the plasma heating effect delays this crossing, weakening the constraints compared to a scenario without it. Thus, Fig. 1 demonstrates that plasma heating allows for a higher neutrino contribution to  $N_{\text{eff}}$  without violating observational bounds, effectively masking additional neutrinos.

We now compare the resulting bounds for Dirac and Majorana neutrinos and examine the impact of including secondary neutrinos.

As previously mentioned, we computed our bounds using two methods: one primarily relying on FRISBHEE with CLASS providing the time-dependent scale factor, and another using CLASS alone. Both methods show excellent agreement at intermediate masses. At low masses,

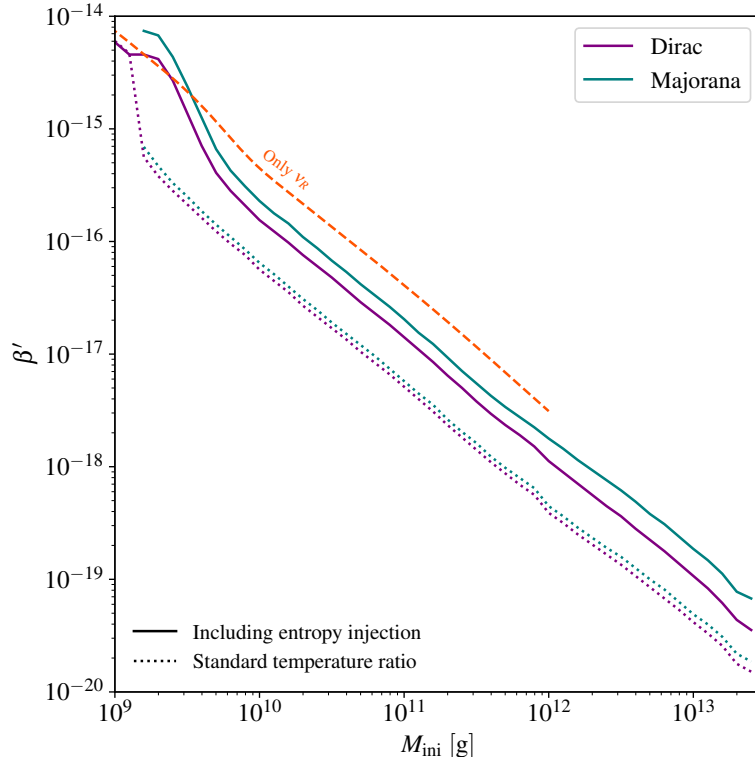


**Figure 2:** Bounds on the abundance of Schwarzschild PBHs of various masses for Dirac (purple) and Majorana (teal) neutrinos, including entropy injection from PBH evaporation (full lines) and neglecting it (dotted lines). Bounds from [64] (including only right-handed neutrinos) are shown for comparison (orange dashed line).

discrepancies arise, as expected, since the CLASS method is less precise in this range due to its treatment of electron-positron annihilation, making FRISBHEE the more reliable approach. At high masses, deviations occur due to matter domination—PBH evaporation begins near or after the onset of matter domination, whereas FRISBHEE assumes radiation domination. Consequently, at high masses, the CLASS method is the more accurate one. Hence, for the bounds presented on Figs. 2 and 3, we select the most reliable method for each mass range, FRISBHEE for  $M < 10^{12}$  g and CLASS for higher masses.

Figure 2 presents the constraints on the initial PBH abundance  $\beta'$  as a function of the initial mass  $M_{\text{ini}}$  for Dirac (purple) and Majorana (teal) neutrinos. The dotted line represents the limits that would be obtained if the modification of the neutrino-photon temperature ratio due to particle injection were not included. As photon and electron emission heats the plasma, the neutrino-photon temperature ratio decreases, leading to a reduction in  $N_{\text{eff}}$ . This effect competes with the increase in  $N_{\text{eff}}$  from neutrino Hawking radiation, ultimately weakening the bounds on  $\beta'$ .

For comparison, the figure also shows bounds from ref. [64], which assume Dirac neutrinos, but only consider the increase in  $N_{\text{eff}}$  due to the emission of right-handed neutrinos, so they do not include the effect of the entropy injection or secondary neutrinos. If we switch off these effects in our calculations, we find good agreement with their results. This comparison shows us that the emission of secondary neutrinos coming from the weak decay of unstable particles significantly strengthens the bounds and reduces the difference between the Dirac

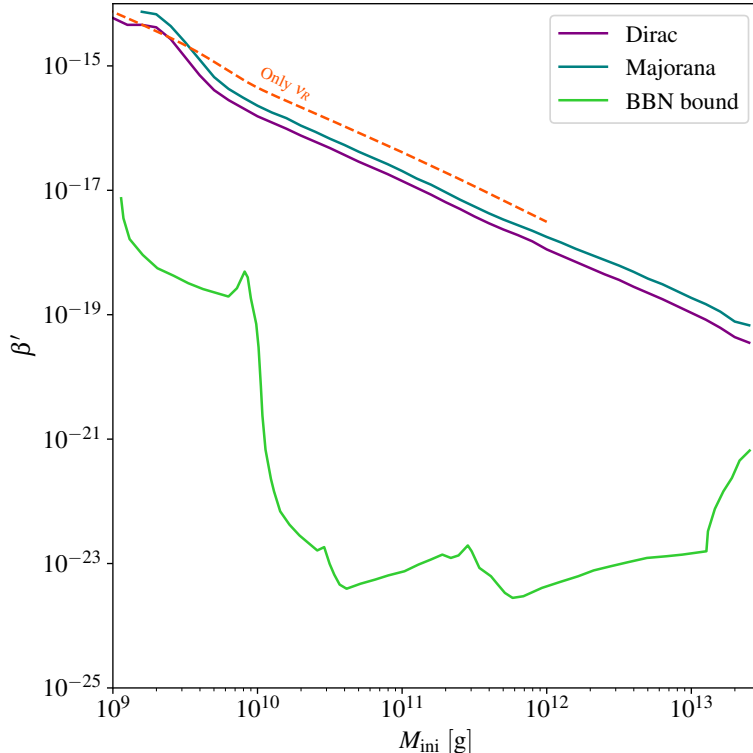


**Figure 3:** Bounds on the abundance of Schwarzschild PBHs of various masses for Dirac (purple) and Majorana (teal) neutrinos coming from  $N_{\text{eff}}$  measurements. For comparison, we show bounds from the same phenomenon that include only right-handed neutrinos, taken from [64] (orange dashed line), as well as bounds coming from Big Bang Nucleosynthesis, taken from [4] (green line).

and Majorana cases. This is expected, as secondary neutrinos originate from weak decays and are exclusively left-handed, making their abundance independent of whether neutrinos are Dirac or Majorana. Since secondary neutrinos dominate the total neutrino emission at these masses, the relative contribution of right-handed neutrinos in the Dirac case becomes less significant.

The temperature ratio effect weakens the constraints on  $\beta'$ , as expected. Note, however, that it does not fully compensate for the strengthening of the bounds due to the effect of secondary neutrinos, so taking both effects into account makes the constraints stricter than ignoring both of them. The effect also increases the difference between the Dirac and Majorana cases. This is intuitive: since the reduction in  $N_{\text{eff}}$  partially offsets the increase from emitted neutrinos, the relative difference in neutrino emission between Dirac and Majorana cases becomes more pronounced.

Figure 3 presents our final bounds, and also compares them with previous bounds from [64] and with BBN bounds from Ref. [4]. Even though our constraints are stricter than previous constraints coming from the same phenomenon, we find that they are less stringent than the BBN bounds, and thus do not exclude any previously allowed region of the PBH parameter space.

We now briefly analyze Kerr PBHs, characterized by the spin parameter  $a_* = J/GM^2$ , where  $J$  is the black hole angular momentum, ranging from 0 (non-rotating) to 1 (maximally

rotating). We computed  $\beta'$  bounds for  $M = 10^{11}$  g, considering cases with and without graviton emission. Graviton emission, expected to be small for non-rotating PBHs but enhanced at high  $a_*$ , should strengthen the bounds by contributing to  $N_{\text{eff}}$ , though its effect remains negligible except at high  $a_*$ , where it slightly lowers the constraints. Overall, while rotation affects the bounds, it at most weakens them by a factor of  $\sim 2$ , and since gravitons remain negligible in realistic cases, the bounds obtained before hold for rotating PBHs with at most an order  $\sim 2$  correction.

## 5 Conclusions

The discovery of primordial black holes (PBHs) would provide a crucial test of their predicted thermal emission. Moreover, a significant population of PBHs evaporating in the early universe could drastically alter cosmological evolution, leading to deviations from standard predictions. This has motivated strong constraints on PBH masses, particularly for those evaporating during Big Bang Nucleosynthesis (BBN) or impacting Cosmic Microwave Background (CMB) observables.

An additional key cosmological probe is the effective number of relativistic species,  $N_{\text{eff}}$ , which has been measured through both BBN and CMB analyses. This observable is influenced by neutrino injection after decoupling and modifications to the neutrino-photon temperature ratio. In this paper, we have examined how a PBH population affects  $N_{\text{eff}}$  through both of these mechanisms.

We have shown that incorporating two additional effects strengthens the bounds on PBH abundance in the mass range  $10^9$  g to  $10^{13}$  g derived from  $N_{\text{eff}}$ . Including neutrino emission from secondary Hawking radiation significantly tightens the constraints, while accounting for the heating of the photon plasma by other emitted particles reduces  $N_{\text{eff}}$  and weakens the bounds. Despite this partial cancellation, our results still yield somewhat stronger limits than those in Ref. [64]. However, our constraints are not the most stringent in this mass range. As shown in Fig. 3, BBN bounds remain considerably stricter, meaning our results do not exclude any previously allowed regions in the PBH parameter space.

The key takeaway from this study is not just the refined bounds but the underlying physics. We have demonstrated that reducing the neutrino-photon temperature ratio can lower  $N_{\text{eff}}$ , allowing additional neutrinos (or other dark radiation components) to be effectively “hidden” without conflicting with observations. This effect could influence constraints on other phenomena, such as dark matter annihilation, where the production of photons or neutrinos depends on branching ratios. Additionally, analyzing spectral distortions in the CMB arising from the interaction of the PBH-emitted neutrinos with the neutrino background may improve the constraints derived here. Exploring these broader implications, however, is beyond the scope of this work and is left for future studies.

## Acknowledgements

GB and HS are supported by the Spanish grants CIPROM/2021/054 (Generalitat Valenciana), PID2023-151418NB-I00 funded by MCIU/AEI/10.13039/501100011033/, and by the European ITN project HIDDeN (H2020-MSCA-ITN-2019/860881-HIDDeN). HS is also supported by the grant FPU23/00257, MCIU. YFPG has been supported by the Consolidación Investigadora grant CNS2023-144536 from the Spanish Ministerio de Ciencia e Innovación (MCIN) and by the Spanish Research Agency (Agencia Estatal de Investigación) through the grant IFT Centro de Excelencia Severo Ochoa No CEX2020-001007-S.

## Appendix A Energy-dependent neutrino interactions

For our calculation of  $N_{\text{eff}}$ , we only consider neutrinos that remain non-interacting after emission, as they contribute to increasing  $N_{\text{eff}}$ . Neutrinos that interact after being emitted can transfer energy to both the neutrino and photon plasma, meaning they do not significantly alter  $N_{\text{eff}}$ , so we exclude them.

In this appendix, we outline the procedure used to determine which neutrinos are excluded due to post-emission interactions. This applies only to left-handed neutrinos, as right-handed neutrinos (if they exist in the Dirac case) do not participate in weak interactions and thus do not thermalize.

Since PBHs emit neutrinos with a spectrum of energies, higher-energy neutrinos have a greater likelihood of interacting. To account for this, we calculate the critical plasma temperature required for a neutrino of a given energy to interact. If a neutrino is emitted when the plasma temperature exceeds this threshold, we assume it interacts and discard it; otherwise, we retain it. We define this threshold as the *energy-dependent decoupling temperature*.

Given that this effect provides only a small correction, we employ an approximate method sufficient to determine the correct order of magnitude. This approach is significantly more precise than simply discarding all neutrinos emitted before standard neutrino decoupling.

A standard way to determine neutrino decoupling is to compare the neutrino scattering rate,  $\Gamma$ , with the Hubble expansion rate,  $H$ . The scattering rate is given by

$$\Gamma = n \langle \sigma v \rangle, \quad (\text{A.1})$$

where  $n$  is the number density,  $\sigma$  is the cross section,  $v$  is the velocity, and  $\langle \dots \rangle$  denotes a thermal average. For relativistic particles, we approximate  $v \approx 1$  and use the Fermi approximation for the cross section,  $\sigma \approx \frac{G_F^2}{\pi} s$ , where  $G_F$  is Fermi's constant and  $s$  is the Mandelstam variable. This approximation holds up to  $s \sim 100$  GeV.

For a PBH neutrino of energy  $E$  interacting with a plasma neutrino of energy  $T$ , assuming a head-on collision, we obtain  $s = 4ET$ . Substituting into  $\Gamma$ , we compare it with the Hubble rate, approximated as  $H \approx T^2/M_P$ , where  $M_P = G^{-1/2}$  is the Planck mass. Setting  $\Gamma \approx H$  gives

$$T_{\text{dec}} = \sqrt{\frac{\pi}{4EM_PG_F^2}}. \quad (\text{A.2})$$

This shows that higher-energy neutrinos decouple at lower plasma temperatures. However, above  $s \sim 100$  GeV, the cross section saturates at  $\sigma \approx \frac{G_F^2}{\pi} M_W^2$ , where  $M_W$  is the W boson mass, leading to a constant decoupling temperature

$$T_{\text{dec}} = \frac{\pi}{M_W^2 M_P G_F^2}. \quad (\text{A.3})$$

Figure 4 shows the energy-dependent decoupling temperature. Neutrinos emitted when the plasma temperature is above their corresponding  $T_{\text{dec}}(E)$  are discarded.

Our results verify that neutrinos of  $\sim 1$  MeV energy decouple at  $\sim 1$  MeV, consistent with standard neutrino decoupling. For higher-energy neutrinos, decoupling occurs significantly later. Since PBHs typically emit neutrinos with energies above 1 MeV, they frequently interact before decoupling. Notably, many of these interactions have sufficient energy to produce electron-positron pairs, injecting energy into the photon plasma rather than the neutrino plasma. This supports our exclusion criterion, as such interactions redistribute energy across both sectors, preventing a significant contribution to  $N_{\text{eff}}$ .

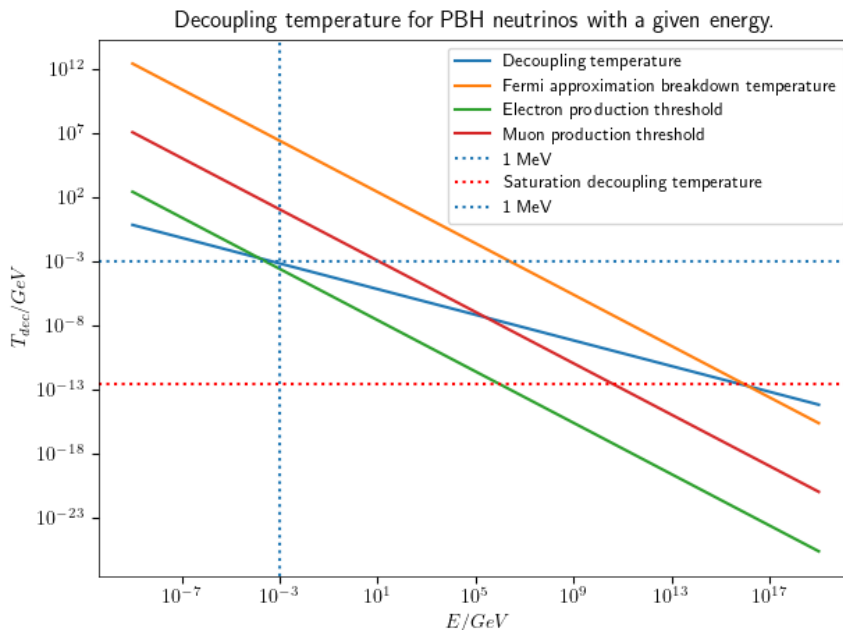


**Figure 4:** Energy-dependent decoupling temperatures where PBH neutrinos no longer interact with plasma neutrinos, assuming the energy of the plasma neutrino equals the plasma temperature (blue solid line). For comparison purposes, we also show the threshold for the interaction to produce an electron-positron pair (green solid line) or a muon-antimuon pair (red solid line), as well as the threshold where the Fermi approximation breaks down (orange solid line) and the saturation value reached after it breaks down (red dashed line). The blue dashed lines show an energy of 1 MeV, which is approximately the standard neutrino decoupling temperature.

## Appendix B Calibration of the spectra

A crucial step in our calculation is calibrating the spectra provided by `BlackHawk`. As noted in its manual, `BlackHawk` outputs spectra assuming a PBH number density of 1 PBH per comoving  $\text{cm}^3$ . Comoving volume remains constant despite cosmic expansion, ensuring consistency in number densities across time.

We introduce the PBH abundance parameter  $\alpha$ , proportional to the PBH abundance, and defined such that  $\alpha = 1$  corresponds to the `BlackHawk` spectra. While the scale factor evolution is inherently included in our integration, we require a global calibration factor to relate  $\alpha$  to the commonly used parameter  $\beta'$ . This is achieved in two steps: first, relating  $\alpha$  to the dark matter fraction parameter  $f$ , and then connecting  $f$  to  $\beta'$ .

We normalize comoving volume to match today's physical volume, setting 1 comoving  $\text{cm}^3$  equal to 1 physical  $\text{cm}^3$  at present. Given that the current dark matter density is approximately  $2 \times 10^{-27} \text{kg}/\text{m}^3$ , which can be obtained from CLASS, we define  $f = 1$  as the case where PBHs constitute all of the dark matter. To simplify calibration, we ignore PBH evaporation and define  $f$  as the fraction assuming PBHs do not evaporate—though not physically realistic, this definition is consistent for our purposes.

For a monochromatic PBH population of mass  $M$ , the PBH number density today is:

$$n_{\text{PBH}}(f = 1) = \frac{\rho_{\text{PBH}}(f = 1)}{M}. \quad (\text{B.1})$$

Since `BlackHawk` assumes  $n_{\text{PBH}}(\alpha = 1) = 1 \text{cm}^{-3}$ , we obtain a mass-dependent relation between  $\alpha$  and  $f$ . The value of  $f$  corresponding to a given  $\alpha$  satisfies  $n_{\text{PBH}}(f(\alpha)) = \alpha \cdot 1 \text{cm}^{-3}$ , while also satisfying  $n_{\text{PBH}}(f(\alpha)) = f(\alpha) \cdot n_{\text{PBH}}(f = 1)$ . Combining these with Eq. (B.1), we derive:

$$f(\alpha) = \frac{\alpha M}{\rho_{\text{PBH}}(f = 1)} \cdot 1 \text{ cm}^{-3}. \quad (\text{B.2})$$

This relation allows us to determine  $f$  for a given  $\alpha$ . To convert  $f$  into  $\beta'$ , we use Eq. (57) from Ref. [4]

$$f \approx 3.81 \times 10^8 \beta' \left( \frac{M}{M_{\odot}} \right)^{-1/2}, \quad (\text{B.3})$$

where  $M_{\odot}$  is the solar mass. Inverting this expression yields:

$$\beta' \approx \left( \frac{M}{M_{\odot}} \right)^{1/2} \frac{f}{3.81 \times 10^8}. \quad (\text{B.4})$$

Thus, this procedure provides a direct relation between  $\alpha$  and  $\beta'$ . Since we obtain spectra from `BlackHawk` for  $\alpha = 1$ , we can derive results for any  $\alpha$  by scaling them accordingly. By linking  $\alpha$  to  $\beta'$ , we obtain results for arbitrary values of  $\beta'$ , enabling our program to place bounds on  $\beta'$ .

## References

- [1] M. Volonteri, M. Habouzit and M. Colpi, The origins of massive black holes, [Nature Reviews Physics](#) **3** (2021) 732 [[2110.10175](#)].
- [2] S.W. Hawking, Black hole explosions, [Nature](#) **248** (1974) 30.
- [3] S.W. Hawking, Particle Creation by Black Holes, [Commun. Math. Phys.](#) **43** (1975) 199.
- [4] B. Carr, K. Kohri, Y. Sendouda and J. Yokoyama, Constraints on Primordial Black Holes, [2002.12778](#).
- [5] B. Carr and F. Kuhnel, Primordial Black Holes as Dark Matter: Recent Developments, [Ann. Rev. Nucl. Part. Sci.](#) **70** (2020) 355 [[2006.02838](#)].
- [6] J. Auffinger, Primordial black hole constraints with Hawking radiation—A review, [Prog. Part. Nucl. Phys.](#) **131** (2023) 104040 [[2206.02672](#)].
- [7] M.Y. Khlopov, Primordial Black Holes, [Res. Astron. Astrophys.](#) **10** (2010) 495 [[0801.0116](#)].
- [8] O. Lennon, J. March-Russell, R. Petrossian-Byrne and H. Tillim, Black Hole Genesis of Dark Matter, [JCAP](#) **04** (2018) 009 [[1712.07664](#)].
- [9] L. Morrison, S. Profumo and Y. Yu, Melanopogenesis: Dark Matter of (almost) any Mass and Baryonic Matter from the Evaporation of Primordial Black Holes weighing a Ton (or less), [JCAP](#) **05** (2019) 005 [[1812.10606](#)].
- [10] D. Hooper, G. Krnjaic and S.D. McDermott, Dark Radiation and Superheavy Dark Matter from Black Hole Domination, [JHEP](#) **08** (2019) 001 [[1905.01301](#)].
- [11] J. Auffinger, I. Masina and G. Orlando, Bounds on warm dark matter from Schwarzschild primordial black holes, [Eur. Phys. J. Plus](#) **136** (2021) 261 [[2012.09867](#)].

- [12] P. Gondolo, P. Sandick and B. Shams Es Haghi, Effects of primordial black holes on dark matter models, *Phys. Rev. D* **102** (2020) 095018 [2009.02424].
- [13] N. Bernal and O. Zapata, Dark Matter in the Time of Primordial Black Holes, *JCAP* **03** (2021) 015 [2011.12306].
- [14] N. Bernal and O. Zapata, Gravitational dark matter production: primordial black holes and UV freeze-in, *Phys. Lett. B* **815** (2021) 136129 [2011.02510].
- [15] N. Bernal and O. Zapata, Self-interacting Dark Matter from Primordial Black Holes, *JCAP* **03** (2021) 007 [2010.09725].
- [16] I. Baldes, Q. Decant, D.C. Hooper and L. Lopez-Honorez, Non-Cold Dark Matter from Primordial Black Hole Evaporation, *JCAP* **08** (2020) 045 [2004.14773].
- [17] I. Masina, Dark matter and dark radiation from evaporating primordial black holes, *Eur. Phys. J. Plus* **135** (2020) 552 [2004.04740].
- [18] I. Masina, Dark Matter and Dark Radiation from Evaporating Kerr Primordial Black Holes, *Grav. Cosmol.* **27** (2021) 315 [2103.13825].
- [19] P. Sandick, B.S. Es Haghi and K. Sinha, Asymmetric reheating by primordial black holes, *Phys. Rev. D* **104** (2021) 083523 [2108.08329].
- [20] N. Bernal, Y.F. Perez-Gonzalez, Y. Xu and O. Zapata, ALP dark matter in a primordial black hole dominated universe, *Phys. Rev. D* **104** (2021) 123536 [2110.04312].
- [21] N. Bernal, F. Hajkarim and Y. Xu, Axion Dark Matter in the Time of Primordial Black Holes, *Phys. Rev. D* **104** (2021) 075007 [2107.13575].
- [22] A. Cheek, L. Heurtier, Y.F. Perez-Gonzalez and J. Turner, Primordial black hole evaporation and dark matter production. I. Solely Hawking radiation, *Phys. Rev. D* **105** (2022) 015022 [2107.00013].
- [23] A. Cheek, L. Heurtier, Y.F. Perez-Gonzalez and J. Turner, Primordial black hole evaporation and dark matter production. II. Interplay with the freeze-in or freeze-out mechanism, *Phys. Rev. D* **105** (2022) 015023 [2107.00016].
- [24] B. Barman, D. Borah, S.J. Das and R. Roshan, Non-thermal origin of asymmetric dark matter from inflaton and primordial black holes, *JCAP* **03** (2022) 031 [2111.08034].
- [25] N. Bernal, Y.F. Perez-Gonzalez and Y. Xu, Superradiant production of heavy dark matter from primordial black holes, *Phys. Rev. D* **106** (2022) 015020 [2205.11522].
- [26] A. Cheek, L. Heurtier, Y.F. Perez-Gonzalez and J. Turner, Evaporation of primordial black holes in the early Universe: Mass and spin distributions, *Phys. Rev. D* **108** (2023) 015005 [2212.03878].
- [27] M. Chen, G.B. Gelmini, P. Lu and V. Takhistov, Primordial black hole neutrino genesis of sterile neutrino dark matter, *Phys. Lett. B* **852** (2024) 138609 [2309.12258].
- [28] M. Chen, G.B. Gelmini, P. Lu and V. Takhistov, Primordial black hole sterile neutrino genesis: sterile neutrino dark matter production independent of couplings, *JCAP* **07** (2024) 059 [2312.12136].
- [29] T. Kim, P. Lu, D. Marfatia and V. Takhistov, Regurgitated Dark Matter, [2309.05703](#).
- [30] M.R. Haque, E. Kpatcha, D. Maity and Y. Mambrini, Primordial black hole versus inflaton, *Phys. Rev. D* **109** (2024) 023521 [2309.06505].
- [31] M. Riajul Haque, E. Kpatcha, D. Maity and Y. Mambrini, Primordial black hole reheating, *Phys. Rev. D* **108** (2023) 063523 [2305.10518].
- [32] A. Chaudhuri, B. Coleppa and K. Loho, Dark matter production from two evaporating PBH distributions, *Phys. Rev. D* **108** (2023) 035040 [2301.08588].

- [33] T.C. Gehrman, B. Shams Es Haghi, K. Sinha and T. Xu, The primordial black holes that disappeared: connections to dark matter and MHz-GHz gravitational Waves, *JCAP* **10** (2023) 001 [[2304.09194](#)].
- [34] T.C. Gehrman, B. Shams Es Haghi, K. Sinha and T. Xu, Recycled dark matter, *JCAP* **03** (2024) 044 [[2310.08526](#)].
- [35] B. Carr, F. Kuhnel and M. Sandstad, Primordial Black Holes as Dark Matter, *Phys. Rev. D* **94** (2016) 083504 [[1607.06077](#)].
- [36] S. Clesse and J. García-Bellido, The clustering of massive Primordial Black Holes as Dark Matter: measuring their mass distribution with Advanced LIGO, *Phys. Dark Univ.* **15** (2017) 142 [[1603.05234](#)].
- [37] B. Carr, M. Raidal, T. Tenkanen, V. Vaskonen and H. Veermäe, Primordial black hole constraints for extended mass functions, *Phys. Rev. D* **96** (2017) 023514 [[1705.05567](#)].
- [38] A.M. Green and B.J. Kavanagh, Primordial Black Holes as a dark matter candidate, *J. Phys. G* **48** (2021) 043001 [[2007.10722](#)].
- [39] D. Croon, D. McKeen, N. Raj and Z. Wang, Subaru-HSC through a different lens: Microlensing by extended dark matter structures, *Phys. Rev. D* **102** (2020) 083021 [[2007.12697](#)].
- [40] J.D. Barrow, E.J. Copeland, E.W. Kolb and A.R. Liddle, Baryogenesis in extended inflation. 2. Baryogenesis via primordial black holes, *Phys. Rev. D* **43** (1991) 984.
- [41] A.S. Majumdar, P. Das Gupta and R.P. Saxena, Baryogenesis from black hole evaporation, *Int. J. Mod. Phys. D* **4** (1995) 517.
- [42] N. Upadhyay, P. Das Gupta and R.P. Saxena, Baryogenesis from primordial black holes after electroweak phase transition, *Phys. Rev. D* **60** (1999) 063513 [[astro-ph/9903253](#)].
- [43] A.D. Dolgov, P.D. Naselsky and I.D. Novikov, Gravitational waves, baryogenesis, and dark matter from primordial black holes, [astro-ph/0009407](#).
- [44] E.V. Bugaev, M.G. Elbakidze and K.V. Konishchev, Baryon asymmetry of the universe from evaporation of primordial black holes, *Phys. Atom. Nucl.* **66** (2003) 476 [[astro-ph/0110660](#)].
- [45] D. Baumann, P.J. Steinhardt and N. Turok, Primordial Black Hole Baryogenesis, [hep-th/0703250](#).
- [46] D. Hooper and G. Krnjaic, GUT Baryogenesis With Primordial Black Holes, *Phys. Rev. D* **103** (2021) 043504 [[2010.01134](#)].
- [47] T.C. Gehrman, B. Shams Es Haghi, K. Sinha and T. Xu, Baryogenesis, primordial black holes and MHz–GHz gravitational waves, *JCAP* **02** (2023) 062 [[2211.08431](#)].
- [48] T. Fujita, M. Kawasaki, K. Harigaya and R. Matsuda, Baryon asymmetry, dark matter, and density perturbation from primordial black holes, *Phys. Rev. D* **89** (2014) 103501 [[1401.1909](#)].
- [49] Y.F. Perez-Gonzalez and J. Turner, Assessing the tension between a black hole dominated early universe and leptogenesis, *Phys. Rev. D* **104** (2021) 103021 [[2010.03565](#)].
- [50] N. Bernal, C.S. Fong, Y.F. Perez-Gonzalez and J. Turner, Rescuing high-scale leptogenesis using primordial black holes, *Phys. Rev. D* **106** (2022) 035019 [[2203.08823](#)].
- [51] S. Jyoti Das, D. Mahanta and D. Borah, Low scale leptogenesis and dark matter in the presence of primordial black holes, *JCAP* **11** (2021) 019 [[2104.14496](#)].
- [52] R. Calabrese, M. Chianese, J. Gunn, G. Miele, S. Morisi and N. Saviano, Limits on light primordial black holes from high-scale leptogenesis, *Phys. Rev. D* **107** (2023) 123537 [[2305.13369](#)].

- [53] R. Calabrese, M. Chianese, J. Gunn, G. Miele, S. Morisi and N. Saviano, Impact of primordial black holes on heavy neutral leptons searches in the framework of resonant leptogenesis, *Phys. Rev. D* **109** (2024) 103001 [2311.13276].
- [54] K. Schmitz and X.-J. Xu, Wash-in leptogenesis after the evaporation of primordial black holes, *Phys. Lett. B* **849** (2024) 138473 [2311.01089].
- [55] A. Ghoshal, Y.F. Perez-Gonzalez and J. Turner, Superradiant leptogenesis, *JHEP* **02** (2024) 113 [2312.06768].
- [56] S. Datta, A. Ghosal and R. Samanta, Baryogenesis from ultralight primordial black holes and strong gravitational waves from cosmic strings, *JCAP* **08** (2021) 021 [2012.14981].
- [57] J. Gunn, L. Heurtier, Y.F. Perez-Gonzalez and J. Turner, Primordial Black Hole Hot Spots and Out-of-Equilibrium Dynamics, [2409.02173](#).
- [58] R. Calabrese, M. Chianese and N. Saviano, The impact of memory-burdened primordial black holes on high-scale leptogenesis, [2501.06298](#).
- [59] T. Papanikolaou, V. Vennin and D. Langlois, Gravitational waves from a universe filled with primordial black holes, *JCAP* **03** (2021) 053 [2010.11573].
- [60] G. Domènech, C. Lin and M. Sasaki, Gravitational wave constraints on the primordial black hole dominated early universe, *JCAP* **04** (2021) 062 [2012.08151].
- [61] N. Bhaumik, A. Ghoshal and M. Lewicki, Doubly peaked induced stochastic gravitational wave background: testing baryogenesis from primordial black holes, *JHEP* **07** (2022) 130 [2205.06260].
- [62] N. Bhaumik, A. Ghoshal, R.K. Jain and M. Lewicki, Distinct signatures of spinning PBH domination and evaporation: doubly peaked gravitational waves, dark relics and CMB complementarity, *JHEP* **05** (2023) 169 [2212.00775].
- [63] A. Ghoshal, Y. Gouttenoire, L. Heurtier and P. Simakachorn, Primordial black hole archaeology with gravitational waves from cosmic strings, *JHEP* **08** (2023) 196 [2304.04793].
- [64] C. Lunardini and Y.F. Perez-Gonzalez, Dirac and Majorana neutrino signatures of primordial black holes, *JCAP* **08** (2020) 014 [1910.07864].
- [65] D. Hooper, G. Krnjaic, J. March-Russell, S.D. McDermott and R. Petrossian-Byrne, Hot Gravitons and Gravitational Waves From Kerr Black Holes in the Early Universe, [2004.00618](#).
- [66] A. Arbey, J. Auffinger, P. Sandick, B. Shams Es Haghi and K. Sinha, Precision calculation of dark radiation from spinning primordial black holes and early matter-dominated eras, *Phys. Rev. D* **103** (2021) 123549 [2104.04051].
- [67] A. Cheek, L. Heurtier, Y.F. Perez-Gonzalez and J. Turner, Redshift effects in particle production from Kerr primordial black holes, *Phys. Rev. D* **106** (2022) 103012 [2207.09462].
- [68] P. Burda, R. Gregory and I. Moss, The fate of the Higgs vacuum, *JHEP* **06** (2016) 025 [1601.02152].
- [69] P. Burda, R. Gregory and I. Moss, Gravity and the stability of the Higgs vacuum, *Phys. Rev. Lett.* **115** (2015) 071303 [1501.04937].
- [70] L. Hamaide, L. Heurtier, S.-Q. Hu and A. Cheek, Primordial black holes are true vacuum nurseries, *Phys. Lett. B* **856** (2024) 138895 [2311.01869].
- [71] M. Ovchinnikov and V. Syvolap, Primordial neutrinos and new physics: novel approach to solving neutrino Boltzmann equation, [2409.15129](#).
- [72] M. Ovchinnikov and V. Syvolap, How new physics affects primordial neutrinos decoupling: Direct Simulation Monte Carlo approach, [2409.07378](#).

- [73] K. Akita, G. Baur, M. Ovchinnikov, T. Schwetz and V. Syvolap, New physics decaying into metastable particles: impact on cosmic neutrinos, [2411.00892](#).
- [74] K. Akita, G. Baur, M. Ovchinnikov, T. Schwetz and V. Syvolap, Dynamics of metastable Standard Model particles from long-lived particle decays in the MeV primordial plasma, [2411.00931](#).
- [75] K. Kohri and J. Yokoyama, Primordial black holes and primordial nucleosynthesis. 1. Effects of hadron injection from low mass holes, *Phys. Rev. D* **61** (2000) 023501 [[astro-ph/9908160](#)].
- [76] C. Keith, D. Hooper, N. Blinov and S.D. McDermott, Constraints on Primordial Black Holes From Big Bang Nucleosynthesis Revisited, *Phys. Rev. D* **102** (2020) 103512 [[2006.03608](#)].
- [77] S.K. Acharya and R. Khatri, CMB and BBN constraints on evaporating primordial black holes revisited, *JCAP* **06** (2020) 018 [[2002.00898](#)].
- [78] A. Boccia, F. Iocco and L. Visinelli, Constraining the primordial black hole abundance through Big-Bang nucleosynthesis, [2405.18493](#).
- [79] A. Arbey and J. Auffinger, Blackhawk: a public code for calculating the hawking evaporation spectra of any black hole distribution, *The European Physical Journal C* **79** (2019) .
- [80] J.H. MacGibbon and B.R. Webber, Quark and gluon jet emission from primordial black holes: The instantaneous spectra, *Phys. Rev. D* **41** (1990) 3052.
- [81] J.H. MacGibbon, Quark and gluon jet emission from primordial black holes. 2. The Lifetime emission, *Phys. Rev. D* **44** (1991) 376.
- [82] J.M. Bardeen, Black Holes Do Evaporate Thermally, *Phys. Rev. Lett.* **46** (1981) 382.
- [83] S. Massar, The Semiclassical back reaction to black hole evaporation, *Phys. Rev. D* **52** (1995) 5857 [[gr-qc/9411039](#)].
- [84] R. Brout, S. Massar, R. Parentani and P. Spindel, A Primer for black hole quantum physics, *Phys. Rept.* **260** (19) 329 [[0710.4345](#)].
- [85] J.D. Bekenstein, Black holes and the second law, *Lett. Nuovo Cim.* **4** (1972) 737.
- [86] J.D. Bekenstein, Black holes and entropy, *Phys. Rev. D* **7** (1973) 2333.
- [87] S.W. Hawking, Breakdown of Predictability in Gravitational Collapse, *Phys. Rev. D* **14** (1976) 2460.
- [88] A. Almheiri, T. Hartman, J. Maldacena, E. Shaghoulian and A. Tajdini, The entropy of Hawking radiation, *Rev. Mod. Phys.* **93** (2021) 035002 [[2006.06872](#)].
- [89] L. Buoninfante, F. Di Filippo and S. Mukohyama, On the assumptions leading to the information loss paradox, *JHEP* **10** (2021) 081 [[2107.05662](#)].
- [90] Y.F. Perez-Gonzalez, Page Time of Primordial Black Holes: Standard Model and Beyond, [2502.04430](#).
- [91] J.D. Barrow, E.J. Copeland and A.R. Liddle, The Evolution of black holes in an expanding universe, *Mon. Not. Roy. Astron. Soc.* **253** (1991) 675.
- [92] E.M. Gutiérrez, F.L. Vieyro and G.E. Romero, Primordial black hole evolution in two-fluid cosmology, *Mon. Not. Roy. Astron. Soc.* **473** (2018) 5385 [[1710.03061](#)].
- [93] E. Dimastrogiovanni and L.M. Krauss,  $\Delta N_{\text{eff}}$  and entropy production from early-decaying gravitinos, *Phys. Rev. D* **98** (2018) 023006 [[1706.01495](#)].
- [94] P.F. de Salas and S. Pastor, Relic neutrino decoupling with flavour oscillations revisited, *JCAP* **07** (2016) 051 [[1606.06986](#)].
- [95] Planck Collaboration, N. Aghanim, Y. Akrami, M. Ashdown, J. Aumont, C. Baccigalupi et al., Planck 2018 results. VI. Cosmological parameters, *A&A* **641** (2020) A6 [[1807.06209](#)].

- [96] M. He, K. Kohri, K. Mukaida and M. Yamada, Formation of hot spots around small primordial black holes, *JCAP* **01** (2023) 027 [[2210.06238](#)].
- [97] M. He, K. Kohri, K. Mukaida and M. Yamada, Thermalization and hotspot formation around small primordial black holes, [2407.15926](#).
- [98] T. Sjöstrand, S. Ask, J.R. Christiansen, R. Corke, N. Desai, P. Ilten et al., An introduction to pythia 8.2, *Computer Physics Communications* **191** (2015) 159–177.
- [99] D. Blas, J. Lesgourgues and T. Tram, The cosmic linear anisotropy solving system (class). part ii: Approximation schemes, *Journal of Cosmology and Astroparticle Physics* **2011** (2011) 034–034.